Autonomous Tilt Rotor Stabilized Plimp Hybrid Airship Unmanned Aerial Vehicle

N. C. Ajay Vishwath, Saras Takearya, Tanishka Mourya, and Ashish Prajapati

1 Literature Review

Moutinho et al. [1] use Lyapunov's theory to analyze nonlinear system stability. Tests have been done to verify the nonlinear performance of controller and thereby correcting the disturbances and errors.

Andan et al. [2] show that the lift force would be three times increased for the airship with wing structure at a positive angle of attack. 20 to 40% of increment in drag occurs with winged airship. Cook et al. [3] explain the various lateral-directional flight modes of the Plimp including modes like sideslip subsidence, yaw subsidence, and oscillatory roll pendulum, also comparison was made between the estimated models and existing airship for various speeds.

DeLaurier et al. [4] performed analysis to develop stability of airships for the non-neutral net buoyancy conditions and non-coincident mass and volumetric centers conditions. Li et al. [5] proposed a method for simulation of airships in nonlinear dynamics. Both the model of the statics and dynamics of air were framed. Wang et al. [6] used CFD and Fourier analysis to obtain the stability derivatives.

Ceruti et al. [7] describe the optimization of airship that consist of two semi-ellipsoids, and axis ratios were altered for the same. The various parameters to optimize were volume, dimension of the tail, ratio between the vertical and the lateral semi-axis, the percentage coverage of photovoltaic films on surface of the top, and the ratio between the longitudinal and the lateral semi-axis. Andan et al. [8] presented the results of a numerical study of aerodynamic parameters for a wingless as well as a winged airship. For various angles, the net force coefficients and moment coefficients have been calculated.

N. C. Ajay Vishwath (✉) · S. Takearya · T. Mourya · A. Prajapati
Parul University, Vadodara 391760, India
e-mail: ajay.nc2934@paruluniversity.ac.in

D. Shukla (ed.), *Lighter Than Air Systems*, Lecture Notes in Mechanical Engineering,
https://doi.org/10.1007/978-981-19-6049-9_15

2 Introduction

The Plimps are the flying devices that can be described as an aircraft with plummet-proof which has lifting capability of an airplane, the thrust control mechanism of a helicopter, and the lift due to buoyancy forces of a Plimp [9]. Egan Airships has designed their eight-passenger Model J. Plimp which are new type of airship, with a combination of helium envelope and dynamic rotors enabled wings, allowing it to perform operations like hovering, dipping, ascending, banking, or spinning [10]. Even at times of engines off mode, it would simply float and glide smoothly to the land. Having VTOL capability, it could lift off from anywhere without runway and land anywhere without runway [11]. The Plimp was initially designed by Daniel P. Raymer, who is a famous expert in the discipline of aircraft conceptual design and aircraft design engineering [12]. Advantage of Plimp being that the aircrafts are noisy, Plimps are not.

3 Design

The pimp would be having a hull, structural frame, thrusters with servos to pivot, the H-tail, and the flight control with an embedded system. The pressurized inflatable envelope would be filled with the suitable gas that is lighter than air that should provide maximum static lift in air for the unmanned aerial airship. Though hull portion of the airship could be shaped with various geometries, the ellipsoidal shaped hull would be preferred for this tilt rotor stabilized hybrid Plimp unmanned aerial vehicle due to high efficiency with less surface area to volume ratio and thereby power consumption could be minimized. This would improve the endurance of the UAV. The tilt rotors would vector the thrust force in necessary directions. Vectoring the thrust components would ease the Plimp to correct its flight path and provide necessary stability in any particular axes. The weight due to gravity, the lift due to aerodynamics, the aerostatic lift, and the thrust vectored lift would be considered as the major force that are acting on this unmanned airship. Among these forces, the aerostatic lift would be given by the differences between the force due to buoyancy and the weight of gas displaced (Fig. 1). Consider volume (V) of the envelope and the density (ρ), the aerostatic lift would be given by

$$\text{Lifting force}\left(L_f\right) = V\left(\rho_{\text{air}} - \rho_{\text{gas}}\right) \tag{1}$$

$$F = m\left(\frac{\mathrm{d}v}{\mathrm{d}t}\right) = \text{Thrust}(F_{\text{t}}) + \text{Buoyancy}(F_{\text{b}}) - \text{Weight}(W)\text{Drag}(F_{\text{d}}) \tag{2}$$

Fig. 1 Free body diagram of takeoff [13]

where

$$\text{Drag}(F_d) = 0.5\, C_D \rho_{air} A v^2 \tag{3}$$

C_D: Drag coefficient and depends on shape,
ρ_{air}: Air density,
A: Area (cross-sectional),
v: Velocity.

The design of envelope has the major impact on the stability, so the necessary design considerations were adopted while designing them. GNVR shape has been chosen to construct the airship. The geometric profile of the airship is given in Fig. 2.

Choice of gas being used I the envelope is also most essential part of the design. So for the comparison, let's tabulate the various gases commonly used along with their densities and molar mass (Table 1).

3.1 Material Selection

Factors affecting the material selection for the envelope; would be the price, the sturdiness, the stress sustaining capability during various flight conditions, including the infiltration of the lifting fluid (gas) [15]. High strength to weight ratio, high tear resistance, resistance to the environmental degradation, and low permeability to LTA gases are the basic material property for choosing such inflatable structure [16, 17]. The biaxial-oriented polyethylene terephthalate in short known as BOPET is selected for inflatable structure material. The metalized BOPET, also known as Mylar, is cheaper than the normal polyurethane. But the studies suggested that it is susceptible to gas (helium) leakage [18]. If the Mylar gets punctured, it would wear out rapidly than the polyurethane material [19].

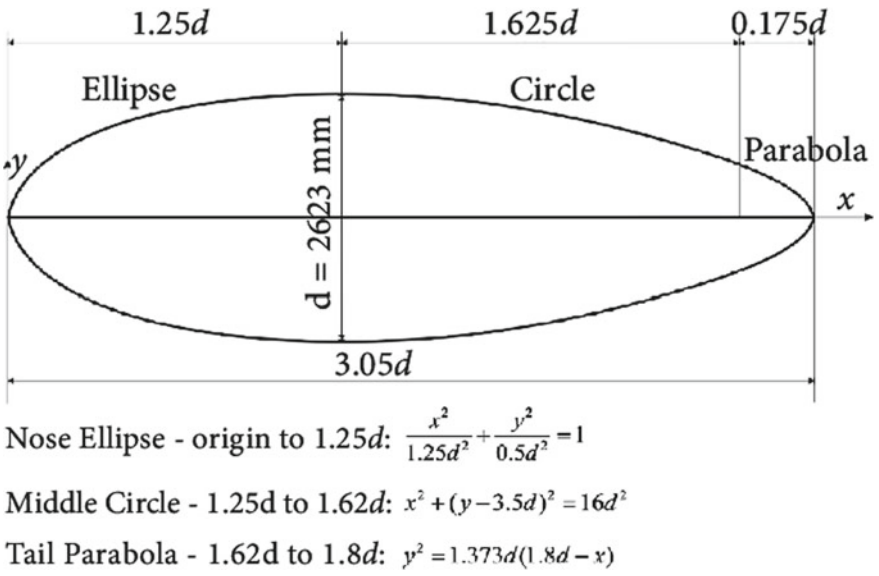

Fig. 2 GNVR profile for the airship [14]

Table 1 Density and molar mass of gases at standard conditions

Gas used in envelope	Density (kg/m^3)	Molar mass (g/mol)
Helium	0.169	4.0026
Methane	0.73	6.04
Ammonia	0.756	17.031
Hydrogen	0.085	2.02
Air	1.225	28.9647

3.2 Stability of Airship

Considering the stability of airships, it could be defined through the classification by static and dynamic. The classification of stability considered during the no powered flight condition would be termed as static stability. The phenomenon of return back to its original position despite of disturbances defines this condition [20] (Table 2).

In general, airships are statically unstable in yaw. Effect of dynamic stability comes in the picture when the airstream flow passes through the control surfaces. Though the stability of airplane and airship seems to have similar classification of stabilities, one of the major differences being that the stabilities in the case of airplanes is associated with one another, but in the case of airships, they being independent of each other. In steady flight, pitch stability, yaw stability, and roll stability are the various stabilities involved.

Table 2 Axes of airship and conventional symbols related to them

Axis		Longitudinal axis	Lateral axis	Normal axis
	Symbol	X	Y	Z
Moment about the axis	Force acting parallel to the axis	X	Y	Z
Angles	Designation	Rolling	Pitching	Yawing
	Symbol	L	M	N
	Positive direction	$Y \rightarrow Z$	$Z \rightarrow X$	$X \rightarrow Y$
Angles	Designation	Roll	Pitch	Yaw
	Symbol	φ	θ	ψ
Velocity components	Linear component about axis	u	V	w
	Angular	p	Q	r

Assumptions that need to be made while performing the derivation of the stability parameters:

(1) The net weight of the body remains constant.
(2) Considering the accessional force to remain constant.
(3) Fixed center of gravity as well as center of buoyancy.
(4) The controls remain in neutral.
(5) Constant velocity.
(6) No changes in the form of airship [20].

3.3 The Various Forces and the Various Moments Acting on the Plimp

Consider Plimp that flying along the horizontal path, such that the flight path makes an angle of 0° with the longitudinal axis, then the various forces and the moments acting on the Plimp would be (see Fig. 3) [20].

(1) Forces

$L_0 =$ Lift of inflating gas acting through center of buoyancy, G.
$W =$ Total weight of dead and live loading, acting through center of gravity, M.
$R =$ Resistance of envelope and appendages, acting through center of pressure, P.
$T =$ Propeller thrust, acting parallel to axis of envelope at distance $o$below$M$.

(2) (2) Moments about M

$Moment L_0 = L_0 \times 0 = 0.$
$Moment W = W \times 0 = 0.$
$Momentthrust - resistancecouple = T(c + d).$

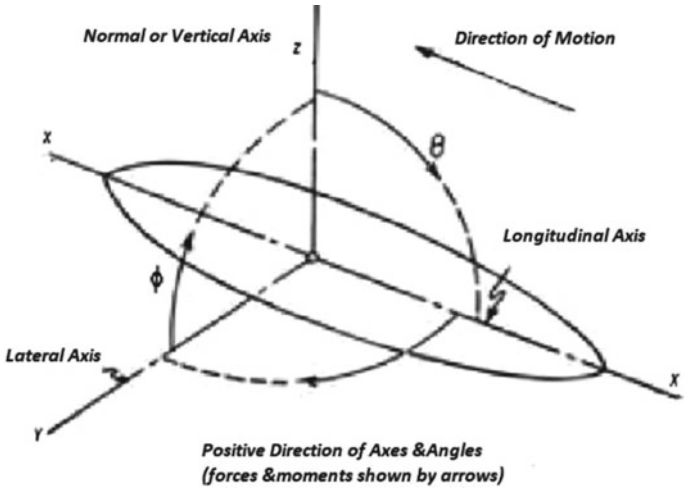

Fig. 3 Axes and angles in positive direction [20]

Condition for static equilibrium and keeping constant velocity

$$L_0 = W \tag{4}$$

$$R = T \tag{5}$$

During the flying condition of Plimp on an even keel, the moments due to thrust force and resistance force would be unbalanced; this would nose up the Plimp. To handle such phenomenon when Plimps are full of gas, are regularly trimmed a few degrees nose heavy. In case of gust, disturbances in the longitudinal axis would give rise to a slight tilt from the horizontal plane, few cases could be observed and described as Table 3.

From Fig. 4, the forces, the lever arms, and the moments, for the cases one to six are noted:

(1) Forces

- L_g = Lifting force of fluid.
- W = The Net Weight acting due to gravity.
- F_e = Resultant air force acting on the envelope.
- L_s = Lift of tail surface.
- F_s = Resultant force acting on the tail surfaces
- T = The thrust of Propeller.
- L_e = Vertical component of the forces due to motion acting on the envelope.
- t = The horizontal component of the thrust produced by propeller .
- R_e = Horizontal component of the forces due to motion acting on the envelope.
- R_s = Drag of the tail surface.

Table 3 Six cases depending on the static state of Plimp with the course of inclination [20]

Case	Static state of airship	Course of inclination
1	Plimp is in the static equilibrium, and nose is tilted up	θ is the angle formed between the direction of motion and longitudinal axis $\theta = 0$ α is the angle between the motion direction and the horizontal, airship climbs at an angle of tilt, α
2	Plimp is in the static equilibrium, and nose is tilted down	$\theta = 0$ and descend angle, α
3	Plimp is statically heavy, and nose is tilted up	Plimp climb at an angle lesser than the angle of tilt, and $(\alpha + \theta)$ will be the angle between longitudinal axis and the horizontal
4	Plimp is statically heavy, and nose is tilted down	$(\alpha - \theta)$ will be the angle between longitudinal axis and horizontal. Plimp descend at an angle greater than the inclination
5	Plimp is statically light, and nose is tilted up	$(\alpha - \theta)$ will be the angle between longitudinal axis and horizontal
6	Plimp is statically light, and nose is tilted down	Plimp descend at an angle lesser than the inclination $(\alpha - \theta)$ will be the angle between longitudinal axis and horizontal

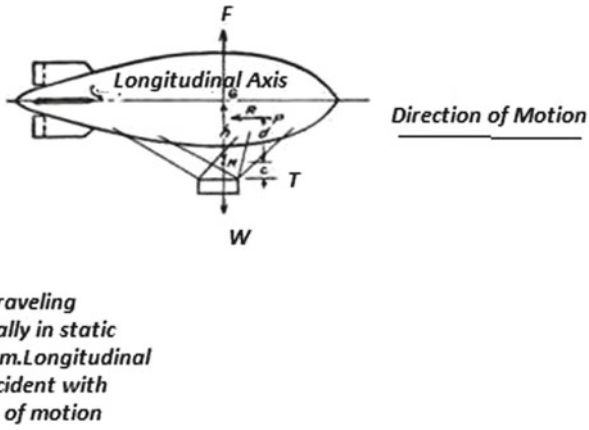

Fig. 4 Forces on airship in horizontal flight [20]

- L_t = The vertical Component of thrust produced by propeller [20].

(2) Leaver Arms

- $W = K \sin(\alpha \pm \theta)$
- $L_g = 0$.

- $T = (c + h)$.
- $F_s = a$(assuming F_s, perpendicular tothe surfaces).
- $L_s = a \times \cos(\alpha \pm \theta)$.
- $R_s = a \times \cos(\alpha \pm \theta)$.
- F_e would vary with the position of P, which in turn would depend on θ.
- $L_e = b \times \cos(\alpha \pm \theta)$.

(3) Moments

- Moment due to weight is $Wh \sin(\alpha \pm \theta)$.
- Moment due to propeller thrust is $T(c + h)$.
- F_e tend to turn the complete Plimp in the positive direction about M due to the increased pressure below the hull. This phenomenon is assisted by reducing the pressure in bottom surface of the tail. The forces acting below the nose of the UAV and the tail of the UAV would be in opposite direction. As the nose force is to some extent is greater than the tail force, there is a difference in force, which will be known as the dynamic lift of hull. Despite of the difference, both the forces have same direction of rotation, and the resultant moment caused is dynamic upsetting moment, denoted by M_e.
- Moment due to the tail surface, denoted by M_s opposes this dynamic upsetting moment. $M_s = L_s \alpha \cos(\alpha \pm \theta) + R_s \alpha \sin(\alpha \pm \theta)$.

3.4 Plimp Stability from Designer Point of View

- Plimps are very stable about their lateral axis.
- Design inputs needed for Plimps to provide longitudinal stability.
- In yaw, Plimps are statically unstable, only pilots can handle this through their rudders.

3.5 Requirements of the Hybrid VTOL Plimp Airship Unmanned Aerial Vehicle

- Payload bay that can carry payload along with the essential electronic components.
- The primary lifting device that would be integrated to the payload bay and installed to provide hydrostatic buoyancy.
- The secondary lifting device integrated to the fuselage and installed to provide dynamic lift through movement of the secondary lifting device through the air.
- The thrust system equipped to generate thrust, the thrust system integrated to the secondary lifting device and it rotates together about an axis that is aligned with the spar of the wing [21].
- The tail system that could be pivoted upon the tail boom to counteract the unwanted forces and moments produced by the tilt rotors [22].

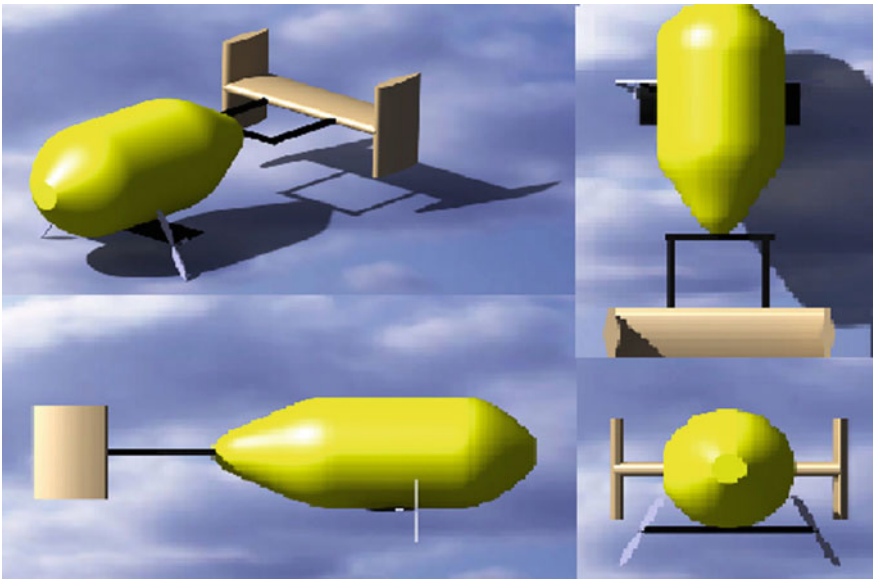

Fig. 5 Isometric, top, side, and front views of Plimp during forward tilt of thrusters

Through the requirements defined above, the hybrid VTOL airship unmanned aerial vehicle with H-tail has been designed using the modeling software CATIA. The various three-dimensional geometric views of the unmanned aerial vehicle are shown in Figs. 5 and 6.

4 Calculations

4.1 Weight Estimation

See Table 4.

4.2 Airfoil Data for the Wing

The airfoil used in this UAV is Bell A821201 (23%) FX-66-H-60, because most of the thrust vector is going to be away from the chord line. This airfoil has flat bottom surface and streamlined upper surface which helps UAV to float stably irrespective of thrust direction.

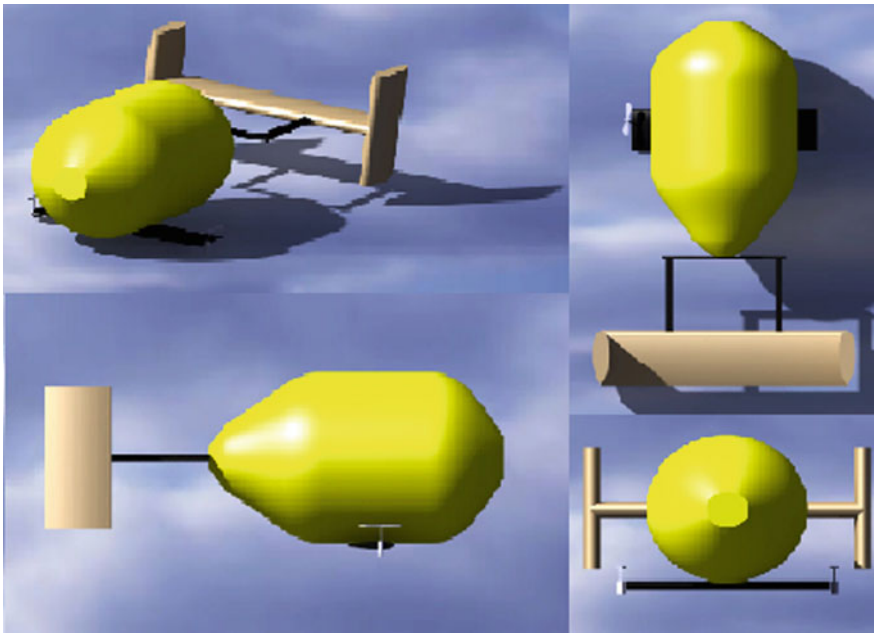

Fig. 6 Isometric, top, side, and front views of Plimp during upward tilt of thrusters

Table 4 Weight estimation of the UAV

Sr no.	Parts	Weight (gm)
1	Envelope with gas	1800
2	BLDC motors	320
3	ESC (2)	80
4	Propellers (2)	40
5	Battery	250
6	Carbon fibertail boom	300
7	Elevator	100
8	Fuselage	200
9	Servo motor (3)	60
10	Receiver	20
11	Extras	130
	Total weight	3300

4.3 Propeller Data

Propeller: Radius 12.7 cm.

$$\text{Area} = \pi r^2 = 0.507\,\text{m}^2 \tag{6}$$

4.4 Different Phases of Flight

Hovering

Calculations of various performance parameters during hovering are given by [23].

Generally, the thrust produced by the motors and the propellers combination should be sufficient to lift the total weight including payload of the UAV

$$T = 2\rho A(V + V_i)V_i = 3.3\,\text{kg} = 32.34\,\text{N} \tag{7}$$

$$V_\text{h} = \sqrt{\frac{W}{2\rho A}} = 16.14\,\text{m/s} \tag{8}$$

$$\Omega = \frac{2\pi N}{60} = 1278.62\,\text{rad/s} \tag{9}$$

$$V_\text{h} = \Omega\, R\sqrt{\frac{C_T}{2}} \tag{10}$$

Thrust of a single BLDC motor with the propeller attached is given by

$$T = C_\text{T}\rho(\Omega R)^2\ A = 32.4265\,\text{N} \tag{11}$$

Torque of a single BLDC motor with the propeller attached is given by

$$Q = C_Q\rho(\Omega R)^2\ AR = 0.5122\,\text{Nm} \tag{12}$$

$$\text{F.O.M} = \frac{C_\text{T}^{3/2}}{\sqrt{2}C_\text{Q}} \tag{13}$$

$$P = Q\ \Omega = 654.89\,\text{Nm/s} \tag{14}$$

Climbing

Calculations of various performance parameters during climbing are given by [23]

$$D = 0.5\,\rho(V + V_i)^2 A_\text{B} C_\text{DB} = 8.9484\,\text{N} \tag{15}$$

$$T = D + W = 41.2936\,\text{N} \tag{16}$$

Therefore,

$$\rho A(V + V_i)2V_i = 0.5\rho(V + V_i)^2 A_{\mathrm{B}} C_{\mathrm{DB}} + W \tag{17}$$

$$Q = 4A(V + V_i)\ \omega R^2 = 1.02097\,\mathrm{Nm} \tag{18}$$

$$Q(\Omega - \omega) = T(V + V_i) \tag{19}$$

$$P = Q\ \Omega = 1305.4327\,\mathrm{Nm} \tag{20}$$

where

V_c is climbing velocity,
D: Drag generated,
AB is the area of the propeller,
C_{D_B} is the drag coefficient due to the propeller.

Forward

Calculations of various performance parameters during forward are given by [23]

$$D = 0.5\ \rho V_{\mathrm{R}}^2 A_{\mathrm{B}} C_{\mathrm{DB}} = 34.7802\,\mathrm{N} \tag{21}$$

$$\tan\delta = \frac{D\cos\varepsilon}{D\sin\varepsilon + W},$$
$$\delta = 46.5301 \tag{22}$$

$$T^2 = D^2 + W^2 + DW\ \sin\varepsilon = 47.822 \tag{23}$$

$$T = 2A\rho V_i\ V_{\mathrm{R}} = 19.2497 \tag{24}$$

$$\mathrm{Q}\ =\ \mathrm{A}\rho V_{\mathrm{R}} R^2\ \omega = 5.1341\,\mathrm{Nm} \tag{25}$$

$$P = Q\,\Omega = 6564.5629\,\mathrm{Nm} \tag{26}$$

5 Mathematical Modeling and Autopilot Control System

The autopilot control system could be developed through modeling the necessary equations that need to be damped from the kinematics of flight [24].

The equations of motion for damping the pitching moments

$$\sum \text{Pitching moments} = \sum M_{\text{cg}} = I_{y\ddot{\theta}} \tag{27}$$

The pitching moment denoted by M and the pitching angle denoted by θ.

M and θ in terms of the initial reference value are mentioned with subscript 0, and the corresponding perturbation is mentioned by Δ

$$M = M_0 + \Delta M \tag{28}$$

$$\theta = \theta_0 + \Delta\theta \tag{29}$$

If case that the reference moment which is denoted by M_0 becomes 0, then the Eq. (27) reduces to

$$\Delta M = I_y \Delta\ddot{\theta} \tag{30}$$

where

$$\Delta M = \frac{\partial M}{\partial \alpha}\Delta\alpha + \frac{\delta M}{\delta \dot{\alpha}}\Delta\dot{\alpha} + \frac{\partial M}{\partial q}\Delta q + \frac{\partial M}{\partial \delta_e}\Delta\delta_e \tag{31}$$

As there is a constrain applied to the C.G, the angle of attack will be identical to the pitch angle

$$\Delta\alpha = \Delta\theta \tag{32}$$

$$\Delta\dot{\theta} = \Delta\dot{\alpha} \tag{33}$$

$$\dot{\theta} = \Delta q \tag{34}$$

After substitution of the expression into Eq. (30), thereby rearranging would yield.

$$\Delta\ddot{\alpha} - \left(M_q - M_{\dot{\alpha}}\right)\Delta\dot{\alpha} + M_\alpha \Delta\alpha = M_{\delta_e}\Delta\delta_e \tag{35}$$

$$M_q = \frac{\partial M/\partial q}{I_y} \tag{36}$$

For the Plimp, the term M_α is negligible and could be eliminated in calculations.

Characteristics equation for Eq. (34) is

$$\lambda^2 - \left(M_q + M_{\dot{\alpha}}\right)\lambda - M_\alpha = 0. \tag{37}$$

The undamped natural frequency ω_n of the system and damping ratio ζ can be determined by

Table 5 Result table of various parameters

Hovering conditions	Climbing conditions	Forward conditions
$V_h = 11.42$ m/s	$V_i = 10.795$ m/s	$V_i = 19.2497$ m/s
$T = 32.34$ N	$T = 41.2936$ N	$T = 47.822$ N
$D =$ Neglected	$D = 8.9484$ N	$D = 34.7802$ N
$Q = 0.5122$ Nm	$Q = 1.02097$ Nm	$Q = 5.1341$ Nm
$P = 654.89$ Nm/s	$P = 1305.4327$ Nm/s	$P = 6564.5629$ Nm/s

$$\omega_n = \sqrt{-M_\alpha} \tag{38}$$

$$\zeta = -\frac{\left(M_q + M_{\dot{\alpha}}\right)}{2\sqrt{-M_\alpha}} \tag{39}$$

For a step change in rudder control, the solution to Eq. (35) would yield a damped sinusoidal motion, considering that the Plimp UAV has enough aerodynamic damping.

6 Results

We have obtained necessary parameters in hovering conditions, climbing conditions, and forward conditions are found out to be Table 5.

When we feed the rudder transfer function in the aircraft transfer function block in the damper block diagram and giving rudder servo equation as $\frac{10}{(S+10)}$.

Washout circuit equation is given by $\frac{s}{s+\frac{1}{\tau}}$ and S (yrg) is given as $1.04\frac{v}{deg/_{sec}}$.

After obtaining the final equation through MATLAB, we use SISO tool toolbar to find the individual root locus and the final stability could be checked through the graph obtained and by varying the gain (Figs. 7, 8, 9, 10, 11, 12 and 13).

7 Summary

A detailed explanation of various design criteria of Plimp hybrid airship unmanned aerial vehicle has discussed along with their definitions and design constraints. Through the inputs of various stability parameters, necessary requirements of the hybrid VTOL Plimp airship have been defined in Sect. 3. The design of the Plimp unmanned aerial vehicle was modeled in CATIA software to get the exact geometric parameters. The calculations for performance parameters after weight estimation were performed in Sect. 4. The detailed calculations for different phases of flight were demonstrated. Further in Sect. 4, a detailed methodology of mathematical

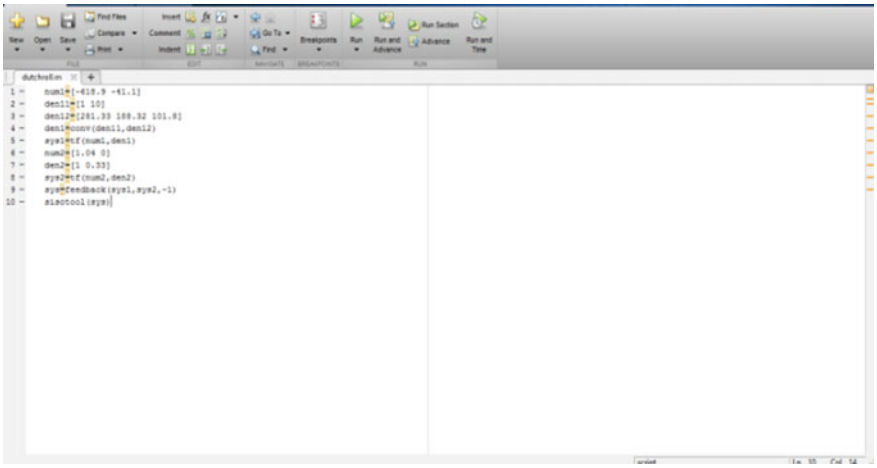

Fig. 7 Program for solving the transfer function MATLAB

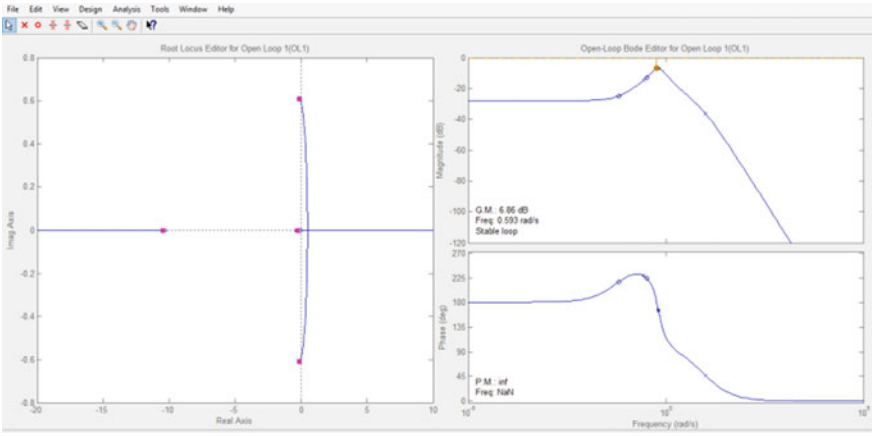

Fig. 8 Graph of the solution for the transfer function in MATLAB

modeling of the stability parameters was derived and necessary equations that would be required for MATLAB code was obtained. In Sect. 5, the coding was performed in MATLAB SISO toolbox and through tuning various gain values, the designed system becomes stable as shown in the graphs of Sect. 6.

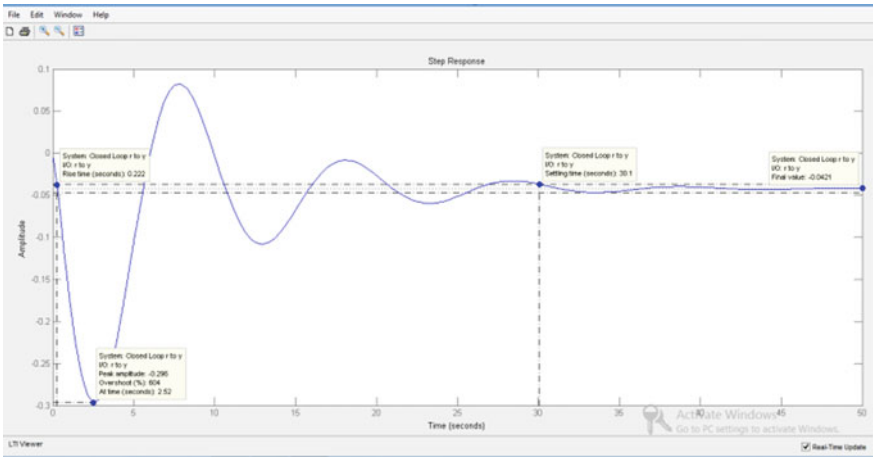

Fig. 9 Step response when gain $k = 1$, damping ratio $= 0.203$, natural frequency $= 0.923$, stable loop [8]

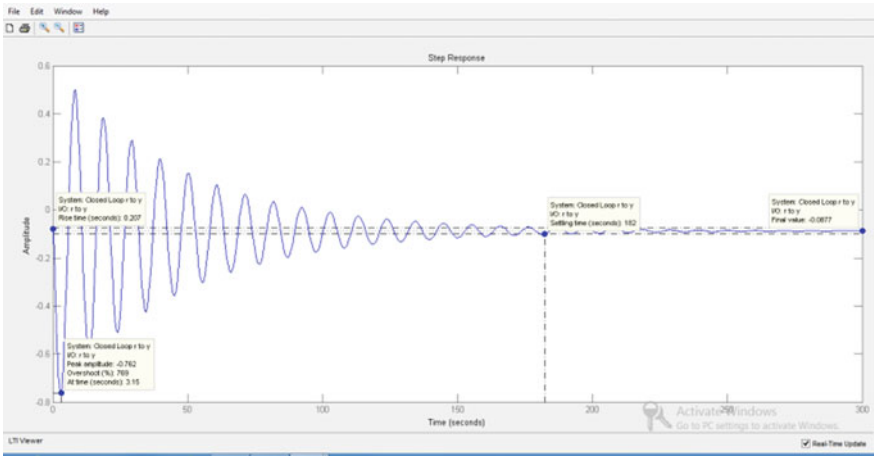

Fig. 10 Step response when gain $k = 3$, damping ratio $= 0.036$, natural frequency $= 0.868$, stable loop

8 Conclusion

The designed tilt rotor stabilized Plimp unmanned aerial vehicle produce enough thrust, torque, and power with least possible drag. Also the MATLAB results show the stability for various gain values with different natural frequencies at various damping ratio. From the graph obtained in MATLAB SISO toolbox, we can see that the disturbances get damped and the system become stable. So this manuscript concludes

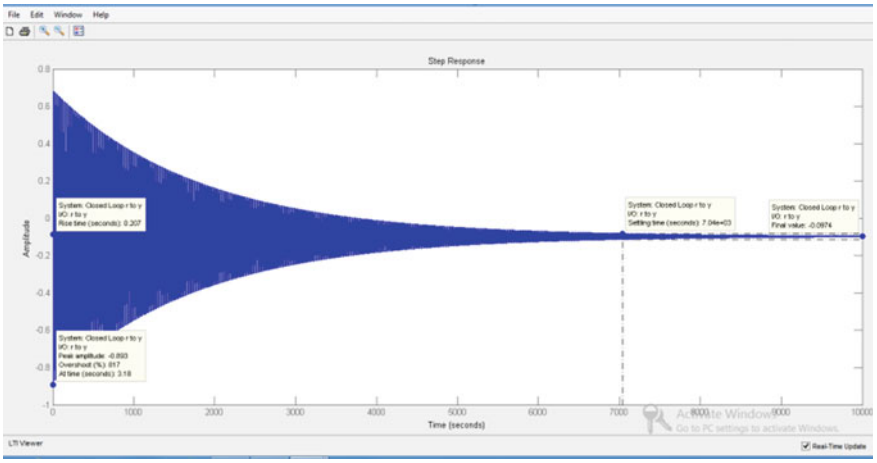

Fig. 11 Step response when gain $k = 3.3$, damping ratio $= 0$, natural frequency $= 0.865$, stable loop

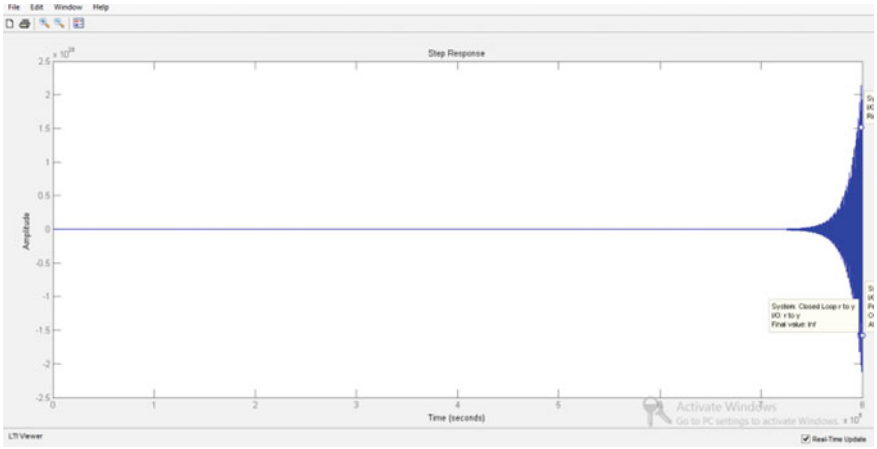

Fig. 12 Step response when gain $k = 3.3$, damping ratio $= -0$, natural frequency $= 0.864$, unstable loop

that the modeled autopilot control system stabilizes the disturbances produced in Plimp hybrid airship UAV.

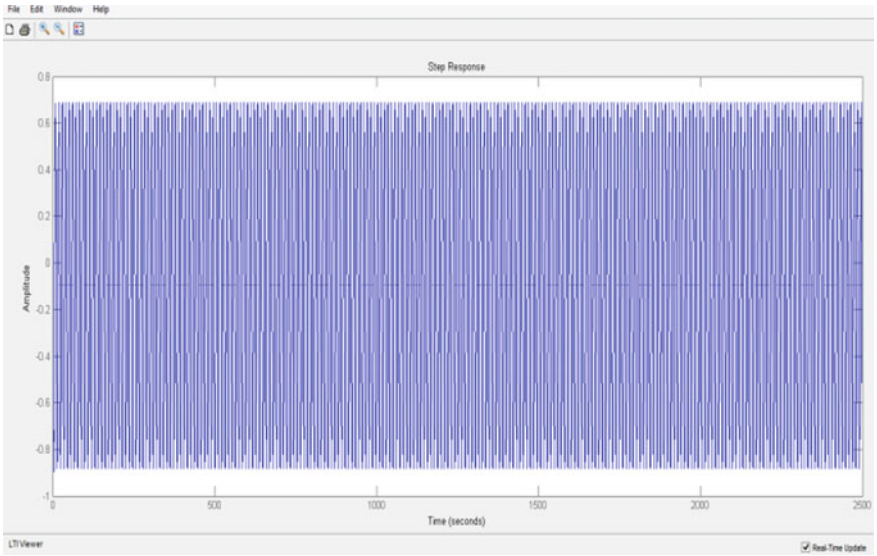

Fig. 13 Step response when gain $k = 3.302651$, damping ratio $= -0$, natural frequency $= 0.864$, neutrally stable loop

References

1. Moutinho Ass, & Azinheira, J. R. Stability and robustness analysis of the AURORA airship control system using dynamic inversion. In Proceedings of the 2005 IEEE International Conference on Robotics and Automation (pp. 2265–2270). Barcelona, Spain(2005, April)
2. Andan AD, Asrar W, Omar AA (2012) Investigation of aerodynamic parameters of a hybrid airship. J Aircr 49(2):658–662
3. Cook MV, Lipscombe JM, Goineau F (2000) Analysis of the stability modes of the non-rigid airship. The aeronautical journal 104(1036):279–290
4. DeLaurier, J., & Schenck, D.). Airship dynamic stability. In 3rd Lighter-Than-Air Systems Technology Conference (p. 1591). (1979)
5. Li Y, Nahon M (2007) Modeling and simulation of airship dynamics. J Guid Control Dyn 30(6):1691–1700
6. Wang XL (2012) Computational fluid dynamics predictions of stability derivatives for airship. J Aircr 49(3):933–940
7. Ceruti A, Voloshin V, Marzocca P (2014) Heusristic algorithms applied to multidisciplinary design optimization of unconventional airship configuration. J Aircr 51(6):1758–1772
8. Andan AD, Asrar W, Omar AA (2012) Aerodynamics of a hybrid airship. In: AIP conference proceedings. Am Inst Phys 1440(1):154–161
9. Hybrid vtol vehicle Homepage. https://patents.google.com/patent/US20160137281/. Last accessed 30 Mar 2022
10. The Plimp airship Homepage. https://www.wearefinn.com/topics/posts/the-plimp-airship-aeroplane-hybrid-is-now-available-to-pre-order/. Last accessed 30 Mar 2022
11. Egan Airships Homepage. https://lynceans.org/wp-content/uploads/2021/04/Egan-Airships_PLIMP_R1-converted.pdf/. Last accessed 30 Mar 2022
12. Dronerush Homepage. https://dronerush.com/blimps-flying-advertisement-drones-10660/. Last accessed 30 Mar 2022

13. Calculating Lifting Capacity of Airships Homepage. https://erik-engheim.medium.com/calculating-lifting-capacity-of-airships-48df5cd7d147/. Last accessed 30 Mar 2022
14. Pant RS (2014) Design, fabrication and flight demonstration of a remotely controlled airship for snow scientists. J Aeros Technol Manag 6:19–27
15. Sadasivan N (2019) Design and realization of an unmanned aerial rotorcraft vehicle using pressurized inflatable structure. Int J Aviat Aeronaut Aeros 6(4):3
16. Miller J, Nahon M (2005) The design of robust helium aerostats. In: AIAA 5th ATIO and 16th lighter-than-air sys technology, and balloon systems conferences. Arlington, Virginia, p 7441
17. Khoury GA (ed) (2012) Airship technology. Cambridge University Press, p 10
18. Nordestgaard M, Ravenscroft L, Bartel N (2007) Design and build a small airship
19. Boon NK (2004) Mini airship patrol craft. National University of Singapore
20. Technical Manual of Airship Aerodynamics Homepage, https://www.faa.gov/regulations_policies/handbooks_manuals/aviation/media/airship_aerodynamics.pdf/. Last accessed 30 Mar 2022
21. Wang X, Cai L (2015) Mathematical modeling and control of a tilt-rotor aircraft
22. Johnson W (1984) Ames research center moffett field, an assessment of the capability to calculate tilting prop-rotor aircraft performance, load and stability, NASA Technical Paper 2291, California
23. Seddon J (1990) PhD, DSc, CEng, CFF, FRA. Blackwell Publications Ltd., Basic Helicopter Aerodynamics
24. Nelson RC (1998) Flight stability and automatic control, 2nd ed. WCB/McGraw Hill, New York